Ion/Ion Reactions in the Gas Phase: Proton Transfer Reactions Involving Multiply-Charged Proteins

James L. Stephenson, Jr., and Scott A. McLuckey*

Contribution from the Chemical and Analytical Sciences Division, Oak Ridge National Laboratory, Oak Ridge, Tennessee 37831-6365

Received April 9, 1996[⊗]

Abstract: Multiply-charged cations derived from electrospray of bovine ubiquitin and horse skeletal muscle apomyoglobin have been subjected to reactions with anions derived from glow discharge ionization of perfluoro-1,3-dimethylcyclohexane. The results are compared with data obtained from proton transfer reactions with strong gaseous neutral bases. Ion/ion reaction rates are shown to be linearly related to the square of the charge on the protein ion, as expected based on a simple capture collision model. Cationic products with charge as low as +1 could be readily formed via ion/ion reactions, whereas efforts to produce such low charge states via ion/molecule reactions have proved unsuccessful. Ion/ion proton transfer reactions appear to be an effective means of reducing charge on highly charged proteins to arbitrarily low charge states. In addition to proton transfer, ion/ion recombination has also been observed. The propensity for proton transfer versus anion attachment to the cation is highly dependent upon the identity of the anion.

Introduction

Several means have recently been developed to form gaseous multiply-charged ions derived from biopolymers and other high mass species. These methods include electrospray[1] (ES), matrix assisted laser desorption,[2] and massive cluster impact.[3] The phenomenon of multiple charging (for which ES is particularly noted) can facilitate the mass measurement of a high mass species by reducing the mass-to-charge ratio to a range of values amenable to mass spectrometry. The distribution of charge states usually produced for high mass species can improve mass measurement precision[1h] by providing multiple mass-to-charge measurements. The multiplicity of ion charge states for individual species, however, can also complicate mass measurement when mixtures of species give rise to ions and for very high mass species. The ability to resolve adjacent charge states for large biopolymers can be the limiting factor in determining the highest mass for which a measurement can be made.

The extent of multiple charging in ES is dependent upon the number of ionizable groups on the molecule,[4] solution conditions[5] (such as pH, solvent, and other solutes), and ES source/interface operating conditions.[6] The charge state distribution has also been shown to be dependent, in some cases, upon biopolymer conformation.[5a,d] Studies aimed at forming ions by ES of relatively low charge from relatively small oligonucleotides have been reported using condensed-phase chemistry strategies with promising results.[7] However, a disadvantage inherent in condensed-phase strategies for charge state reduction is that the ionization process can be compromised. It is therefore desirable to decouple ionization from the charge state reduction process. An example of such an approach is the use of strong gaseous bases, present in either an interface region[8] or high vacuum of the mass spectrometer,[9] to deprotonate multiply-protonated species. It has been demonstrated that strong gaseous bases deprotonate highly charged proteins at rates near the predicted collision rates but the reactions become increasingly slow (inefficient) as charge state decreases.[9] Proton transfer reaction exoergicity is expected to decrease with protein charge

[⊗] Abstract published in *Advance ACS Abstracts,* August 1, 1996.

(1) (a) Yamashita, M.; Fenn, J. B. *J. Phys. Chem.* **1984**, *88*, 4451−4459. (b) Yamashita, M.; Fenn, J. B. *J. Phys. Chem.* **1984**, *88*, 4671−4675. (c) Aleksandrov, M. L.; Gall, L. N.; Krasnov, N. V.; Nikolaev, V. I.; Paulenko, V. A.; Shkurov, V. A. *Dokl. Phys. Chem. (Engl.)* **1984**, *277*, 572−575. (d) Wong, S. F.; Meng, C. K.; Fenn, J. B. *J. Phys. Chem.* **1988**, *92*, 546−550. (e) Meng, C. K.; Mann, M.; Fenn, J. B. *Z. Phys. D.: At. Mol. Clusters* **1988**, *10*, 361−368. (f) Fenn, J. B.; Mann, M.; Meng, C. K.; Wong, S. F.; Whitehouse, C. M. *Science* **1990**, *246*, 64−71. (g) Smith R. D.; Loo, J. A.; Edmonds, C. G.; Barinaga, C. J.; Udseth, H. R. *Anal. Chem.* **1990**, *62*, 882−899. (h) Fenn, J. B.; Mann, M.; Meng, C. K.; Wong, S. F.; Whitehouse, C. M. *Mass Spectrom. Rev.* **1990**, *9*, 37−70. (i) Smith, R. D.; Loo, J. A.; Ogorzalek Loo, R. R.; Busman, M.; Udseth, H. R. *Mass Spectrom. Rev.* **1991**, *10*, 359−451. (j) Mann, M. *Org. Mass Spectrom.* **1990**, *25*, 575−587. (k) Huang, E. C.; Wachs, T.; Conboy, J. J.; Henion, J. D. *Anal. Chem.* **1990**, *62*, 713A−725A.

(2) (a) Karas, M.; Hillenkamp, F. *Anal. Chem.* **1988**, *60*, 2299−2301. (b) Overberg, A.; Karas, M.; Hillenkamp, F. *Rapid Commun. Mass Spectrom.* **1991**, *5*, 128−131. (c) Nordhoff, E.; Ingedoh, A.; Cramer, R.; Overberg, A.; Stahl, B.; Karas, M.; Hillenkamp, F.; Crain, P. F. *Rapid Commun. Mass Spectrom.* **1992**, *6*, 771−776.

(3) (a) Mahoney, J. F.; Perel, J.; Ruatta, S. A.; Martino, P. A.; Husain, S.; Lee, T. D. *Rapid Commun. Mass Spectrom.* **1991**, *5*, 441−445. (b) Mahoney, J. F.; Perel, J.; Lee, T. D.; Martino, P. A.; Williams, P. *J. Am. Soc. Mass Spectrom.* **1992**, *3*, 311−317.

(4) (a) Covey, T. R.; Bonner, R. F.; Shushan, B. I.; Henion, J. *Rapid Commun. Mass Spectrom.* **1988**, *2*, 249−256. (b) Smith R. D.; Loo, J. A.; Edmonds, C. G.; Barinaga, C. J.; Udseth, H. R. *Anal. Chem.* **1990**, *62*, 882−899.

(5) (a) Chowdhury, S. K.; Katta, V.; Chait, *J. Am. Chem. Soc.* **1990**, *112*, 9012−9013. (b) Guevremont, R.; Siu, K. W. M.; Leblanc, J. C. Y.; Berman, S. S. *J. Am. Soc. Mass Spectrom.* **1992**, *3*, 216−224. (c) Feng, R.; Konishi, Y. *J. Am. Soc. Mass Spectrom.* **1993**, *4*, 638−645. (d) Loo, J. A.; Loo, R. R. O.; Udseth, H. R.; Edmonds, C. G.; Smith, R. D. *Rapid Commun. Mass Spectrom.* **1991**, *5*, 101−105. (e) Katta, V.; Chait, B. T. *Rapid Commun. Mass Spectrom.* **1991**, *5*, 214.

(6) (a) Loo, J. A.; Udseth, H. R.; Smith, R. D. *Rapid Commun. Mass Spectrom.* **1990**, *4*, 207. (b) Ashton, D. A.; Reddell, C. R.; Cooper, D. J.; Green, B. A.; Oliver, R. W. A. *Org. Mass Spectrom.* **1993**, *28*, 721−718. (c) Leblanc, J. C. Y.; Beuchemin, D.; Siu, K. W. M.; Guevremont, R.; Berman, S. S. *Org. Mass Spectrom.* **1991**, *26*, 831−839. (d) Mirza, U. A.; Cohen, S. L.; Chait, B. T. *Anal. Chem.* **1993**, *65*, 1−6.

(7) Cheng, X.; Gale, D. C.; Udseth, H. R.; Smith, R. D. *Anal. Chem.* **1995**, *67*, 586−593.

(8) (a) Ikonomou, M. G.; Kebarle, P. *Int. J. Mass Spectrom. Ion Processes* **1992**, *117*, 283−298. (b) Loo, R. R. O.; Udseth, H. R.; Smith, R. D. *J. Phys. Chem.* **1991**, *95*, 6412−6415. (c) Winger, B. E.; Light-Wahl, K. J.; Smith, R. D. *J. Am. Soc. Mass Spectrom.* **1992**, *3*, 624−630. (d) Loo, R. R. O.; Loo, J. A.; Udseth, H. R.; Fulton, J. L.; Smith, R. D. *Rapid Commun. Mass Spectrom.* **1992**, *6*, 159−165. (e) Winger, B. E.; Light-Wahl, K. J.; Rockwood, A. L.; Smith, R. D. *J. Am. Chem. Soc.* **1992**, *114*, 5897−5898. (f) Loo, R. R. O.; Smith, R. D. *J. Am. Soc. Mass Spectrom.* **1994**, *5*, 207−220. (g) Ogorzalek-Loo, R. R.; Winger, B. E.; Smith, R. D. *J. Am. Soc. Mass Spectrom.* **1994**, *5*, 1064−1071.

for a given protein/base combination. The reactions can become endoergic for low charge state proteins even with the strongest of neutral gaseous bases. Furthermore, clustering often competes with proton transfer at low charge states giving rise to an increase in mass, rather than a decrease in charge.[9] The point at which proton transfer becomes inefficient and if and when clustering becomes competitive depend upon the nature of the protein, the nature of the base, and reaction conditions, such as temperature and pressure. The detailed roles of these factors are not yet well understood making an *a priori* prediction of reaction rates difficult. Based on studies performed to date with strong neutral gaseous bases, ion/molecule reactions do not appear to provide means for reducing charge states to arbitrarily low values.

We have recently reported on the reactions of multiply charged anions with singly charged cations in a Paul trap.[10] Examples involving proton transfer, electron transfer, and recombination have been described. We have recently adapted a Paul trap to allow for the study of multiply charged cations with singly charged anions.[11] The present study was undertaken to address the extent to which high mass multiply-protonated species can be de-protonated with singly charged anions, and to determine the rate dependence of these reactions on cation charge. In contrast with ion/neutral reactions, ion/ion reactions are expected to be exoergic for all combinations of charge states. Ion/ion reactions might therefore be exploited for the partial neutralization of multiply-charged ions to arbitrarily low charge states.

Experimental Section

Samples and Apparatus. The proteins ubiquitin and horse skeletal muscle myoglobin were obtained from Sigma Chemical Co., St. Louis, MO. Perfluorodimethyl-1,3-cyclohexane (PDCH), 1,6-hexanediamine, and the proton sponge (*N*,*N*,*N*′,*N*′-tetramethyl-1,8-naphthalenediamine) were obtained from Aldrich, Milwaukee, WI, and dimethylamine was obtained from ChemService, West Chester, PA. Solutions for electrospray were prepared by dissolving the sample in 5 mL to give a concentration of 20 μM in at least 4:1 methanol:water (v/v). All solutions were infused at rates of 1.0−3.0 μL/min through a 120 μm i.d. needle held at a potential of +3500 to +4000 V.

All experiments were carried out with a home-made electrospray source coupled with a Finnigan-MAT (San Jose, CA) Ion Trap Mass Spectrometer modified for injection of ions formed external to the ion trap through an end-cap electrode. Details of the electrospray/ion trap interface have been described.[12] Further modifications have been made to this apparatus to allow anions to be injected through a 3 mm diameter hole drilled through the ring electrode. Details of these modifications and others made to facilitate analysis of high mass-to-charge ions will be reported elsewhere.[11] A brief description of the hardware changes is given here.

An atmospheric sampling glow discharge ion source[13] has been mounted on a side port of a 6 in. cube used to support the ion trap assembly. The ion trap is situated such that there is a line of sight from the exit aperture of the glow discharge ion source to the 3-mm hole in the ring electrode. A lens stack is mounted off of the glow discharge ion source to facilitate ion transport to the ring electrode. The discharge is pulsed under software control[14] via a high voltage solid state pulser (Directed Energy Inc., Fort Collins, CO, Model GRX-1.5K-E). The output of the pulser is connected to the anode of the glow discharge source. The pulser acts as a fast switch which alternates between a voltage sufficient to strike a discharge (≈−400 V, as normally provided by an ORTEC Oak Ridge, TN, Model 556 power supply) and ground. This arrangement allows for independent control of cation accumulation and anion accumulation. The glow discharge provides a convenient means for forming a wide variety of singly charged anions in high abundance. In all cases, the multiply-charged protein ions were accumulated prior to anion accumulation.

For the case of ion/molecule proton transfer reactions involving cations of horse skeletal muscle apomyoglobin, the gaseous base was admitted into the unheated vacuum system to a pressure of $1-5 \times 10^{-7}$ Torr. These experiments consisted of a cation accumulation period, followed by a delay of 100−400 ms prior to mass analysis. No detailed kinetic measurements of individual charge states were undertaken. In the case of the kinetic measurements of ion/ion reactions involving individual charge states of ubiquitin, a mass selection step was used after cation accumulation (see below) to select the charge state of interest. An anion accumulation period of 15 ms was used to admit anions followed by a delay period of variable duration to allow for the measurement of parent cation loss as a function of time. Ion/ion reaction rates were determined by measuring the loss rate of the parent ions of the selected charge state. The rate was obtained from the slope of the plot of the negative logarithm of the I_t/I_0 intensity ratio versus time. Pseudo-first-order kinetics prevail due to the great excess of anions over cations present in the ion trap during the reaction period.

Ion Manipulation and Mass/Charge Analysis. Cations were injected axially into the ion trap for periods ranging from 0.1 to 0.2 s. The radio frequency (rf) sine-wave amplitude applied to the ring electrode during ion injection ranged from 700 to 1200 V zero-to-peak. In all cases, helium was admitted into the vacuum system to a total pressure of 1 mTorr with a background pressure in the instrument of 2×10^{-5} Torr without the addition of helium. Anions were formed by sampling the head space vapors of PDCH into the glow discharge operated at 800 mTorr.

Details of ion isolation for high-mass multiply-charged ions have been given previously.[15] A single resonance ejection scan was used for isolation of parent ions. Low *m*/*z* ions were ejected by passing the ions through a q_z value of 0.908 by scanning the amplitude of the ring-electrode rf sine-wave. High *m*/*z* ions were ejected by dipolar resonance ejection scan using a 12-V p−p sine-wave signal applied to the end caps at a frequency selected to eject ions at an *m*/*z* value slightly greater than that of the parent ion. Parent ions were isolated prior to the anion accumulation period at less than unit resolution to avoid parent ion loss, due either to dissociation or to ejection from off-resonance power absorption.

Mass/charge analysis was effected after the completion of all ion isolation and reaction periods using resonance ejection[16] to yield a mass/charge range (for apomyogobin) as high as 22 000 using resonance ejection amplitudes of 3−4 V p−p. The mass/charge scale for the ion/ion reaction spectra was calibrated initially using the electrospray mass spectrum of the parent compound. In this work, the mass/charge ratios of the various charge states of the parent compound were known

(9) (a) McLuckey, S. A.; Van Berkel, G. J.; Glish, G. L. *J. Am. Chem. Soc*. **1990**, *112*, 5668−5670. (b) McLuckey, S. A.; Glish, G. L.; Van Berkel, G. J. *Anal. Chem*. **1991**, *63*, 1971−1978. (c) Cassady, C. J.; Wronka, J.; Kruppa, G. H.; Laukien, F. H. *Rapid Commun. Mass Spectrom*. **1994**, *8*, 394−400. (d) McLuckey, S. A.; Goeringer, D. E. *Anal. Chem*. **1995**, *67*, 2493−2497. (e) Schnier, P. D.; Gross, D. S.; Williams, E. R. *J. Am. Chem. Soc*. **1995**, *117*, 6747−6757. (f) McLuckey, S. A.; Van Berkel, G. J.; Glish, G. L.; Schwartz, J. C. In *Modern Mass Spectrometry: Practical Aspects of Ion Trap Mass Spectrometry*; March, R. E., Todd, J. F. J., Eds.; CRC Press: Boca Raton, 1995; Vol. 2, Chapter 3, 89−141. (g) Cassady, C. J.; Carr, S. R. *J. Mass Spectrom*. **1996**, *31*, 247−254.

(10) (a) Herron, W. J.; Goeringer, D. E.; McLuckey, S. A. *J. Am. Soc. Mass Spectrom*. **1995**, *6*, 529−532. (b) Herron, W. J.; Goeringer, D. E.; McLuckey, S. A. *J. Am. Chem. Soc*. **1995**, *117*, 11555−11562. (c) Herron, W. J.; Goeringer, D. E.; McLuckey, S. A. *Anal. Chem*. **1996**, *68*, 257−262. (d) Herron, W. J.; Goeringer, D. E.; McLuckey, S. A. *Rapid Commun. Mass Spectrom*. **1996**, *10*, 277−281.

(11) Stephenson, J. L., Jr.; McLuckey, S. A. In *Int. J. Mass Spectrom. Ion Processes*. In press.

(12) (a) Van Berkel, G. J.; McLuckey, S. A.; Glish, G. L. *Anal. Chem*. **1990**, *62*, 1284−1295. (b) McLuckey, S. A.; Van Berkel, G. J.; Glish, G. L.; Huang, E. C.; Henion, J. D. *Anal. Chem*. **1991**, *63*, 375−383.

(13) (a) McLuckey, S. A.; Glish, G. L.; Asano, K. G.; Grant, B. C. *Anal. Chem*. **1988**, *60*, 2220−2228. (b) McLuckey, S. A.; Glish, G. L.; Asano, K. G. *Anal. Chim. Acta* **1989**, *225*, 25−35. (c) Eckenrode, B. A.; Glish, G. L.; McLuckey, S. A. *Int. J. Mass Spectrom. Ion Processes* **1990**, *99*, 151.

(14) ICMS software provided by N. Yates and the University of Florida.

(15) McLuckey, S. A.; Goeringer, D. E.; Glish, G. L. *J. Am. Soc. Mass Spectrom*. **1991**, *2*, 11−21.

(16) (a) Kaiser, R. E., Jr.; Cooks, R. G.; Moss, J.; Hemberger, P. H. *Rapid Commun. Mass Spectrom*. **1989**, *3*, 50−53. (b) Kaiser, R. E., Jr.; Louris, J. N.; Amy, J. W.; Cooks, R. G. *Rapid Commun. Mass Spectrom*. **1989**, *3*, 225−229.

and could be used to determine a correction for the mass scale provided by the ion trap data system. As charges were removed and the mass scale was extended, calibrations were made in a stair-step fashion. The mass/charge ratios of ions which were measured at a lower mass range extension factor were used to determine the new mass range extension factor when the mass range was extended further. In this way, the mass scale associated with the largest mass range extension factor could be related back to the original mass scale calibration. The spectra shown here were typically the result of an average of 50−100 individual scans.

Results and Discussion

In considering the role of charge in the rates of ion/ion proton transfer reactions it is useful to refer to a model that predicts the ion/ion collision rate as a function of charge. If it is assumed that ion/ion proton transfer reactions involving multiply-protonated proteins proceed via a long-lived collision complex, a rate constant for a capture collision, k_c, can be derived in direct analogy with derivations for ion/molecule orbiting collisions.[17] Treating the oppositely charged ionic reactants as structureless point charges,[18] by far the most important potential at long range is the attractive Coulomb potential, rather than the ion−dipole and ion−induced dipole interactions that apply in ion/molecule collisions. Ignoring the internal energies of the reactants, the total energy of the collision pair, E_{tot}, is the sum of potential, E_{pot}, and kinetic, E_{kin}, energies, i.e.

$$E_{tot} = E_{pot} + E_{kin} \tag{1}$$

The instantaneous system kinetic energy at any given interparticle separation, r, can be divided further into translational and rotational components, viz.,

$$E_{kin}(r) = E_{trans}(r) + E_{rot}(r) \tag{2}$$

The dominant potential at long range for ion/ion collisions is the Columb potential, such that

$$E_{tot} = \frac{-Z_1Z_2e^2}{r} + E_{rot}(r) + E_{trans}(r) \tag{3}$$

where e is the electron charge and Z_1 and Z_2 are numbers of charges on the cation and anion, respectively. The instantaneous rotational kinetic energy is given by

$$E_{rot}(r) = \frac{\mu v^2 b^2}{2r^2} \tag{4}$$

where μ is the reduced mass of the collision pair, v is the relative velocity, and b is the classical impact parameter. This energy is the so-called "centrifugal barrier" that opposes the attractive potential and is associated with non-zero impact parameter collisions. It is therefore often added to the attractive potential to give an effective potential, $V_{eff}(r)$. In the case of ion/ion reactions this is

$$V_{eff}(r) = \frac{-Z_1Z_2e^2}{r} + \frac{\mu v^2 b^2}{2r^2} \tag{5}$$

The maximum impact parameter that leads to an orbiting collision, the critical impact parameter b_c, is that corresponding to the point at which the maximum $V_{eff}(r)$ is equal to the total relative energy of the collision pair, $^1/_2\mu v^2$. This is given by

$$\frac{\partial V_{eff}(r)}{\partial r} = 0 = \frac{Z_1Z_2e^2}{r^2} - \frac{\mu v^2 b^2}{r^3} \tag{6}$$

The critical ion/ion separation, r_c, which applies to an orbiting complex formed from a collision at the critical impact parameter, is

$$r_c = \frac{\mu v^2 b_c^{\,2}}{Z_1Z_2e^2} \tag{7}$$

The critical impact parameter is related to the critical ion/ion separation by

$$b_c = 2^{1/2} r_c \tag{8}$$

which, when substituted into (7), gives

$$r_c = \frac{Z_1Z_2e^2}{2\mu v^2} \tag{9}$$

and

$$b_c = \frac{2^{1/2}Z_1Z_2e^2}{2\mu v^2} \tag{10}$$

The cross section for ion/ion capture, σ_c, is given by

$$\sigma_c = \left(\frac{\pi}{2}\right)\left[\frac{Z_1Z_2e^2}{\mu v^2}\right]^2 \tag{11}$$

The rate constant for ion/ion capture, k_c, is given by

$$k_c = v\sigma_c = v\left(\frac{\pi}{2}\right)\left[\frac{Z_1Z_2e^2}{\mu v^2}\right]^2 \tag{12}$$

Using units of cm/s for relative velocity, grams for reduced mass, unit charges for Z_1 and Z_2, and electrostatic units for e yields σ_c and k_c in units of cm^2 and cm^3/s, respectively. As a basis for comparison, the ion/molecule capture collision rate derived from pure polarization theory takes the form

$$k_{c(I/M)} = 2\pi Z(\alpha/\mu)^{1/2} \tag{13}$$

where α represents the polarizability of the neutral reactant. Note that there are several significant differences in the dependencies of the rate constant for capture for ion/ion reactions (eq 12) and for ion/molecule reactions (eq 13) on Z, v, and μ. Of particular note for this work is the predicted Z^2 dependence of k_c on both anion and cation charge for ion/ion reactions compared with a linear dependence upon Z for $k_{c(I/M)}$.

Equations 12 and 13 are useful as simple models for predicting the rates at which collision partners collide but provide no insight into the dynamics that determine if a collision leads to a reaction. Given the significant differences in the

(17) (a) Langevin, P. M. *Ann. Chim. Phys.* **1905**, *5*, 245. (b) Eyring, H.; Hirschfelder, J. O.; Taylor, H. S. *J. Chem. Phys.* **1936**, *4*, 479. (c) Gioumousis, G.; Stevenson, D. P. *J. Chem. Phys.* **1958**, *29*, 294. (d) Su, T.; Bowers, M. T. In *Gas Phase Ion Chemistry*; Bowers, M. T., Ed.; Academic Press: New York, 1979; Vol. 1, Chapter 3. (e) Su, T.; Bowers, M. T. *Int. J. Mass Spectrom. Ion Phys.* **1973**, *12*, 347. (f) Su, T.; Bowers, M. T. *Int. J. Mass Spectrom. Ion Phys.* **1975**, *17*, 211. (g) Chesnavich, W. J.; Su, T.; Bowers, M. T. *J. Chem. Phys.* **1980**, *72*, 2641. (h) Su, T.; Bowers, M. T. *J. Chem. Phys.* **1982**, *76*, 5183.

(18) The point charge assumption becomes increasingly inaccurate as the ion−ion separation distance decreases. A pair-wise treatment of the ion−ion attraction is necessary to model the interaction potential at short range. Furthermore, polarization, particularly of the anion, may be important at short range. However, the point charge treatment closely approximates the interaction potential at maximum distances for capture.

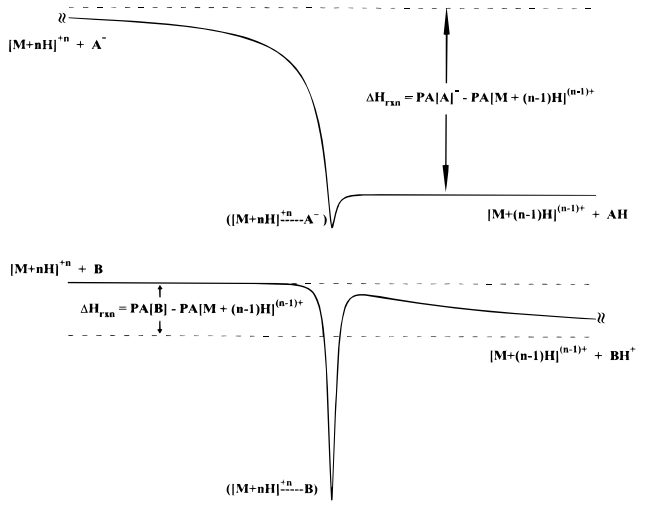

Figure 1. Generic energy diagrams (a) for an ion−ion proton transfer reaction and (b) for an ion−molecule proton transfer reaction.

energy surfaces over which ion/ion and ion/molecule reactions proceed, it is useful to highlight the differences in these reaction types to provide a context for interpretation of the results presented here. Figure 1 shows generic energy diagrams for the ion/ion proton transfer reaction

$$MH_n^{n+} + A^- \rightarrow MH_{(n-1)}^{(n-1)+} + AH \qquad (14)$$

and for the ion/molecule proton transfer reaction

$$MH_n^{n+} + B \rightarrow M_{(n-1)}^{(n-1)+} + BH^+ \qquad (15)$$

drawn in analogy with the Brauman diagram[19] frequency used to represent proton transfer reactions. The entrance channel for the ion/ion reaction is dominated by the long-range attractive $-Z_1Z_2e^2/r$ potential whereas the products, once formed, must overcome ion−dipole and ion−induced dipole potentials to proceed over the exit channel. The enthalpy of the reaction is determined by the difference in the proton affinity (PA) of $MH_{(n-1)}^{(n-1)+}$ and the proton affinity of A^- (or its equivalent, the gas-phase acidity of AH), i.e.

$$\Delta H_{rxn} = PA(A^-) - PA(MH_{(n-1)}^{(n-1)+}) \qquad (16)$$

While relatively little is known about proton affinities of cations,[20] deprotonation of even the strongest of gaseous bases by singly charged anions is expected to be exothermic since there is a significant gap in energy between the highest proton affinities of neutral bases and the lowest proton affinities of anions. The effect of multiple protonation is to reduce the stabilization associated with the addition of each successive proton. Therefore, deprotonation via reaction 14 is expected to be exothermic for every value of *n*.

In the case of ion/molecule proton transfer reactions, reaction enthalpy is determined by the difference between the proton affinities of B and $PA(MH_{(n-1)}^{(n-1)+})$, viz.

$$\Delta H_{rxn} = PA(B) - PA(MH_{(n-1)}^{(n-1)+}) \qquad (17)$$

Since $PA(A^-) \gg PA(B)$ in general, reaction 14 is always more likely to be exothermic than reaction 15. However, the energy surface associated with the ion/molecule reaction may also reduce the rate of reaction 15 by making it endoergic even if it is slightly exothermic overall. The entrance channel for the multiply-charged ion/molecule reaction is governed at long range by attractive polarization forces whereas the exit channel, in which two products of like charge are formed, is dominated by a repulsive $+Z_1Z_2e^2/r$ potential at long range. This creates a barrier in the exit channel the magnitude of which is determined by the strength of the Coulomb field at the transition state. This situation has important implications in the ion/molecule chemistry associated with multiply-charged ions and has been discussed within the context of the chemistry of both small multiply-charged ions[21] and high mass multiply-charged ions.[9] No such Coulomb barrier applies to reaction 14, however, because there is no separation of like charges on the energy surface.

The foregoing arguments support the expectation that ion/ion reactions might be more effective at reducing the charge on a multiply protonated protein than ion/molecule reactions. However, previous studies in which multiply charged protein ions were merged at atmospheric pressure with ions of opposite polarity in a Y-tube arrangement leading to the sampling aperture of a mass spectrometer did not provide clear evidence to support this expectation.[22] While shifts from higher charge states to lower charge states and reductions in total ion signal were noted, no examples were reported of shifts as great as have been observed by ion/molecule reactions. Several other interesting observations were made, however, suggesting the transfer of two protons on a single collision between a multiply-charged protein and a singly-charged anion and enhancement of solvation associated with the merged ions in the Y-tube. Due to the relatively complex set of reaction conditions prevalent in the Y-tube studies, inherent ion/ion reactivity could not be evaluated unambiguously. The present studies provide for better defined reaction conditions and reflect ion/ion reactivity in the dilute gas phase.

Figure 2 compares results obtained by storing multiply-protonated ions derived from horse skeletal muscle myoglobin in the presence of various gas-phase bases. Figure 2a shows the spectrum derived from storing the myoglobin ions in the presence of 5×10^{-7} Torr of dimethylamine (PA = 220.6 kcal/mol)[23] for 100 ms whereas Figures 2b and 2c show results acquired for roughly 400 ms reaction time using 1×10^{-7} Torr of 1,6-hexanediamine (PA = 237.7 kcal/mol)[23] and the proton sponge (PA = 241.8 kcal/mol),[23] respectively. (In the case of the proton sponge experiment, mass analysis conditions were such that the protonated base, the other product of reaction 15, was also apparent in the spectrum.) In each case, very little change in charge state distribution occurs at longer storage times (not shown) indicating that the rate constants for proton transfer for the charge states shown in the figures are far lower than the collision rate. In all three cases, a significant change in charge state distribution is noted from the charge state distribution observed in the absence of base (see Figure 3a), which shows a distribution of charge of $n = 9-23$ with the most abundant ions appearing with charges $n = 15-18$. The extent to which charge is reduced increases with the proton affinity of the gaseous base, as has also been observed in the much lower

(19) Jasinski, J. M.; Brauman, J. I. *J. Am. Chem. Soc.* **1980**, *102*, 2906−2913.

(20) See ref 9e and: Kaltashov, I. A.; Fenselau, C. C. *J. Am. Chem. Soc.* **1995**, *117*, 9906−9910.

(21) (a) Tonkyn, R.; Weisshaar, J. C. *J. Am. Chem. Soc.* **1986**, *108*, 7128−7130. (b) Roth, L. M.; Freiser, B. S. *Mass Spectrom. Rev.* **1991**, *10*, 303−328. (c) Petrie, S.; Javahery, G.; Wincel, H.; Bohme, D. K. *J. Am. Chem. Soc.* **1993**, *115*, 6290−6294. (d) Javahery, G.; Petrie, S.; Wincel, H.; Wang, J.; Bohme, D. K. *J. Am. Chem. Soc.* **1993**, *115*, 6295−6301.

(22) (a) Loo, R. R. O.; Udseth, H. R.; Smith, R. D. *J. Phys. Chem.* **1991**, *95*, 6412−6415. (b) Loo, R. R. O.; Udseth, H. R.; Smith, R. D. *J. Am. Soc. Mass Spectrom.* **1992**, *3*, 695−705.

(23) Lias, S. G.; Bartmess, J. E.; Liebman, J. F.; Holmes, J. L.; Levin, R. D.; Mallard, W. G. *J. Phys. Chem. Ref. Data* **1988**, *17*, *Suppl. No. 1*.

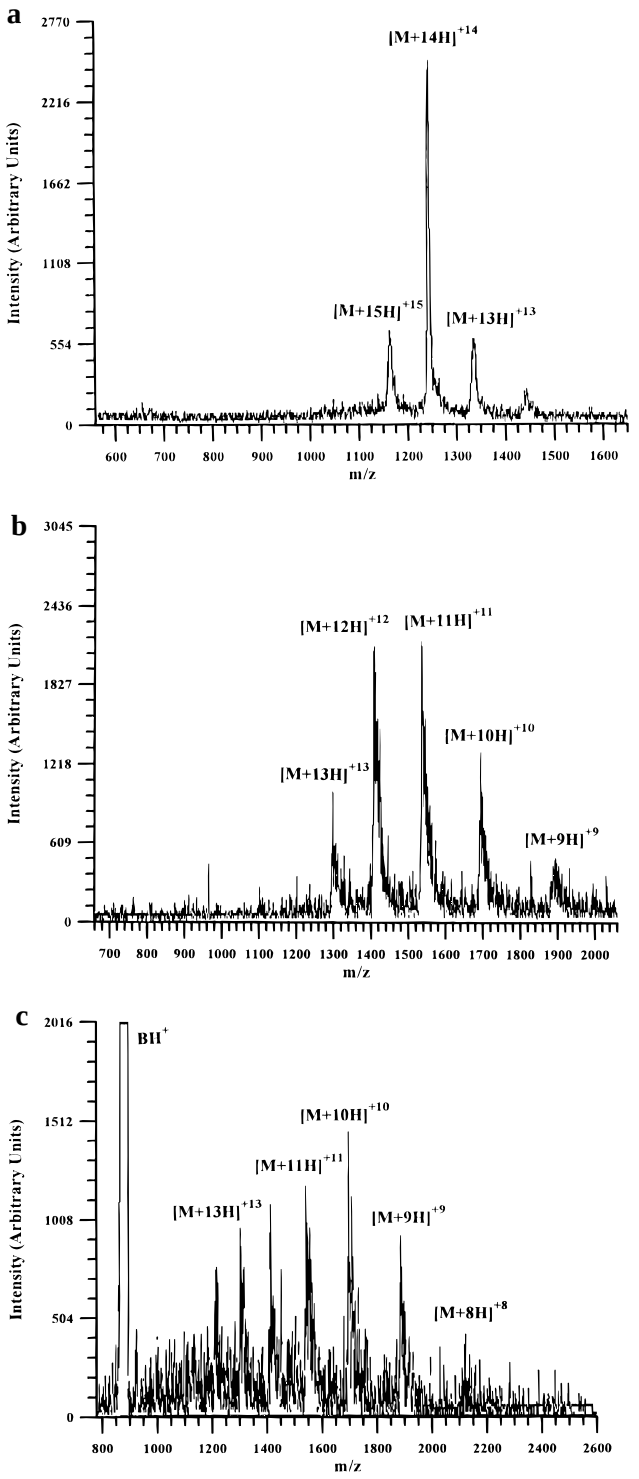

Figure 2. ES ion−molecule reaction spectra of horse skeletal myoglobin (a) with 5×10^{-7} Torr of dimethylamine for 100 ms, (b) with 1×10^{-7} Torr of 1,6-hexanediamine for 400 ms, and (c) with 1×10^{-7} Torr of proton sponge for 400 ms.

pressure environment of the ion cyclotron resonance mass spectrometer.[9c,e] This observation is consistent with the interpretation that reaction exoergicity increases with base strength thereby reducing the charge states at which the reactions become endoergic or nearly so. It is also noteworthy that careful inspection of peak shapes and positions indicated that clustering also contributed to the peak shapes in Figure 2. It has already been noted that clustering tends to compete with proton transfer in the ion trap operated and helium bath gas at 1 mTorr when proton transfer rates become low.[9b,f] Somewhat less clustering has been noted in ion cyclotron resonance studies with similar

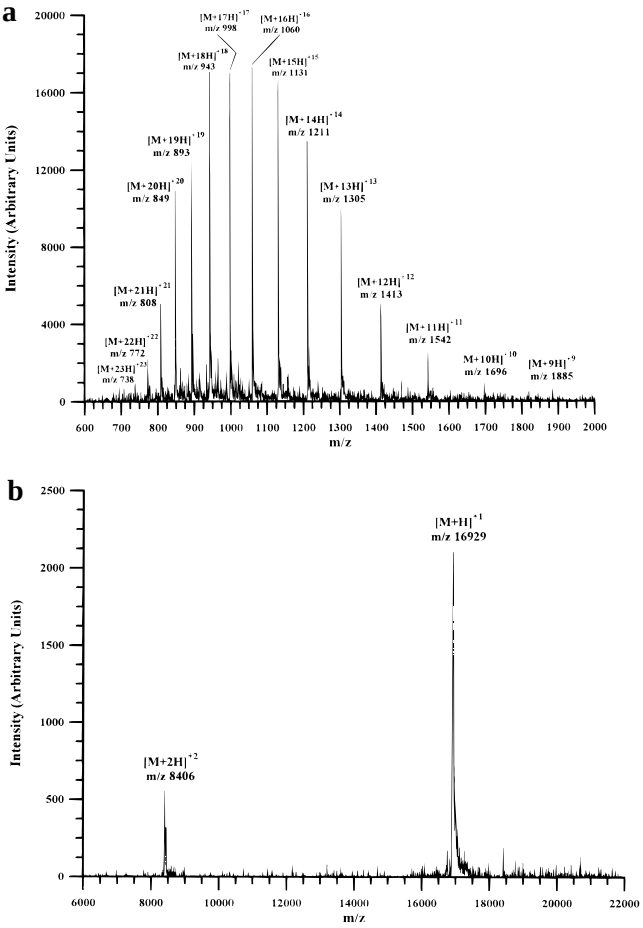

Figure 3. ES mass spectrum of horse skeletal myoglobin (a) with no anions present in the trapping volume to produce a charge distribution ranging from +23 to +9 and (b) after a 330-ms reaction with PDCH anions which reduced the charge state distribution to primarily the +2 and +1 charge states.

systems, perhaps due to the lower likelihood for three-body collisions that could stabilize a cluster ion. Furthermore, somewhat greater shifts in charge state have been noted, perhaps due to the lesser competition due to clustering. In any case, Figure 2 is included here to show the extent to which multiply-protonated apomyoglobin can be deprotonated in the ion trap using strong neutral bases under reaction conditions similar to those used to effect ion/ion reactions.

Figure 3 shows the electrospray mass spectrum of horse skeletal muscle myoglobin in the absence of either anions or neutral bases (Figure 3a) and after the ions have been subjected to reactions with anions derived from PDCH for 330 ms (30 ms anion accumulation plus 300 ms mutual storage). Glow discharge ionization of PDCH and anion injection through the ring electrode yields intense anions at *m*/*z* 381 and 331 corresponding to $(M-F^{\bullet})^-$ and $(M-CF_3^{\bullet})^-$, respectively. These anions were injected into the ion trap using a low *m*/*z* cutoff of 50 and the mutual storage time employed a low *m*/*z* cutoff of 150. Clearly, under these reaction conditions ion/ion proton transfer reactions can reduce the charge on apomyoglobin to significantly lower levels than can ion/molecule reactions using very strong neutral bases under ion trap reaction conditions. Indeed, we have noted that apomyoglobin charge can be readily reduced to +1 using several combinations of anion accumulation time and mutual storage time.[24] These data are illustrative of every multiply-charged peptide and protein that we have studied thus far, including a variety of doubly- and triply-charged peptides, bovine insulin, and bovine albumin. In the latter case, poor signals are observed for the lowest charge states due to

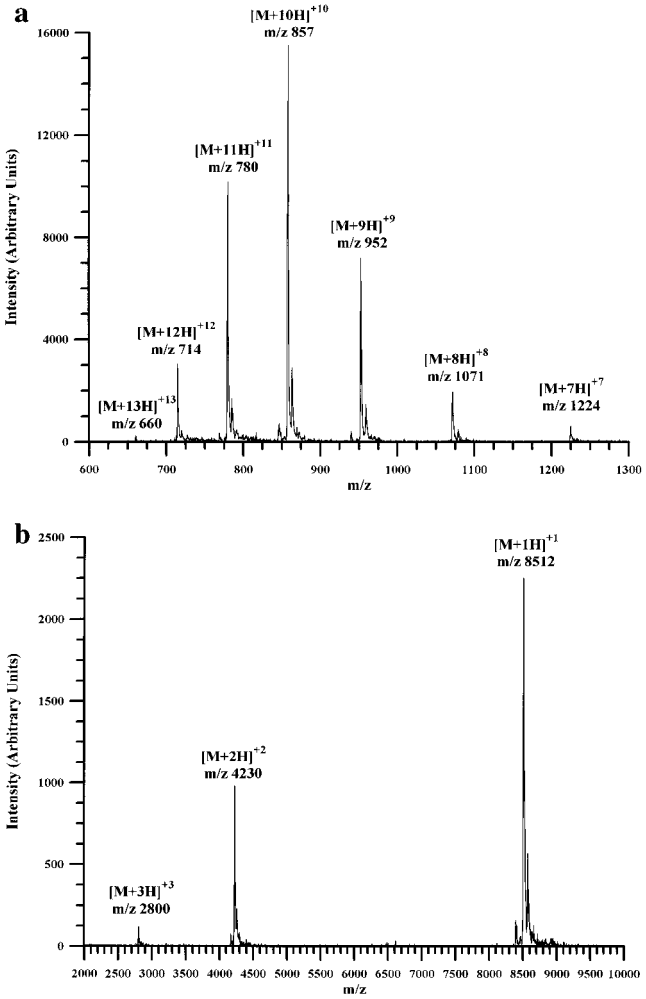

Figure 4. ES mass spectrum of Bovine red blood cell ubiquitin (a) with no anions present in the trapping volume to produce a charge distribution ranging from +13 to +7 and (b) after a 305-ms reaction with PDCH anions which reduced the charge state distribution to primarily the +3, +2, and +1 charge states.

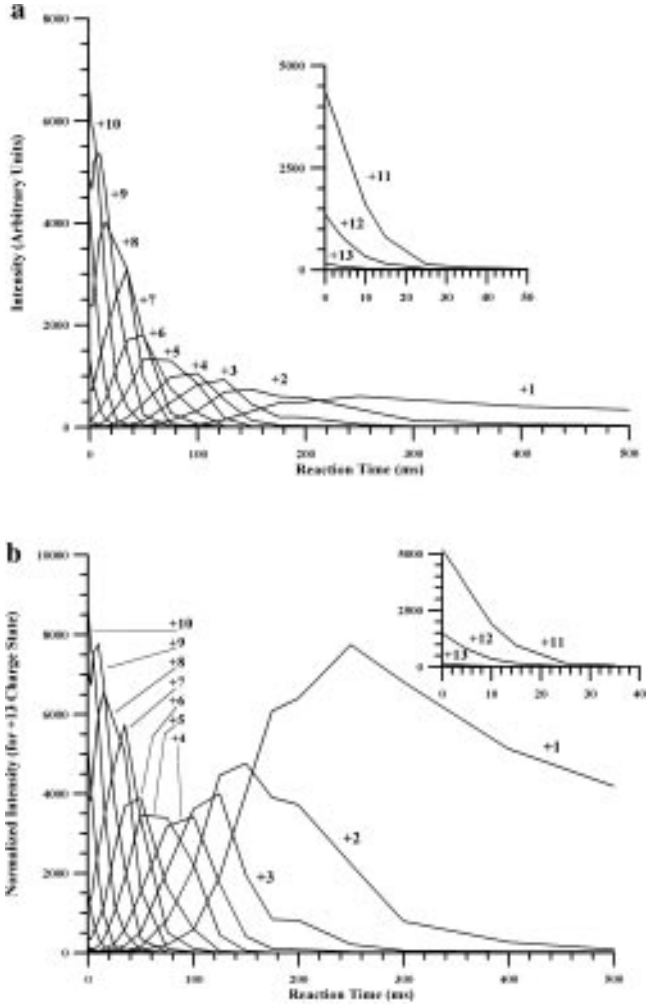

Figure 5. Consecutive reaction curves for the reaction of bovine red blood cell ubiquitin with PDCH anions for a fixed 15 ms anion accumulation time, and a variable mutual storage time; (a) uncorrected plot showing the inherent width of the charge state distributions as they are detected at a rate proportional to charge state and (b) corrected plot showing normalized signal levels where each curve is multiplied by 13/*n*.

limitations in ion storage and detection at *m*/*z* values in excess of 3×10^4. Nevertheless, a singly-charged ion derived from a globular protein (bovine albumin) with initial charge states in the range of $n = 35-50$ was measured following a reaction period of 500 ms.[25]

We chose to evaluate the relationship between ion/ion reaction rate and charge state using cations derived from ubiquitin and anions derived from PDCH. Ubiquitin was selected in part because ion/molecule kinetic data for a large fraction of ubiquitin charge states with a variety of strong gaseous bases has been reported by Cassady et al. using an ion cyclotron resonance mass spectrometer.[9c] These results provide an important set of quantitative data for comparing and contrasting ion/ion and ion/molecule proton transfer kinetics.

Figure 4 compares the electrospray mass spectrum of ubiquitin (part a) with the spectrum resulting from interaction of the protonated ubiquitin ions with the PDCH anions for 305 ms (30 ms anion accumulation and 275 ms mutual storage time). A summary of the time evolution associated with these reactions is given in Figure 5, which shows a plot of the signals associated with the various ubiquitin charge states as a function of reaction time (15 ms anion accumulation, variable mutual storage time). The plot of Figure 5a shows the data uncorrected for the inherent width of the *m*/*z* distributions associated with the various charge states. As charge increases, the isotopic distribution of the protein is compressed into a narrower range of *m*/*z*. At a fixed rate of scan of the amplitude of the drive rf, therefore, the ions are ejected to the detector at a rate in proportion to charge state. Since the signal intensity is directly related to current, higher charge states give greater signal heights than an equal number of ions in a lower charge state[26] due to the fact that the population of ions of the higher charge state are ejected from the ion trap and into the detector at a higher rate. Figure 5b shows the same plot normalized for effective scan rate by multiplying signals levels by the factor 13/*n*. This plot gives a more accurate picture of ion losses associated with the ion/ion reactions than does Figure 5a but does not account for the dependence of detector response on charge state. We therefore conclude that ion losses are relatively minor in the experiments

(24) Anion accumulation time is related to the anion number density available for reaction. The rate of reaction is therefore affected by the anion accumulation time such that various combinations of anion accumulation time and mutual storage time can result in the same extent of reaction.

(25) Stephenson, J. L., Jr.; McLuckey, S. A., Unpublished Results, Oak Ridge National Laboratory, 1996.

(26) Note that this effect is independent of the number of charges on the ion. The detector may also have a different response for equal numbers of ions with different numbers of charges. See, for example: (a) Axelsson, J.; Reimann, C. T.; Sundqvist, B.U.R. *Int. J. Mass Spectrom. Ion Processes* **1994**, *133*, 141−155. (b) Loo, J. A.; Pesch, R. *Anal. Chem.* **1994**, *66*, 3659−3663.

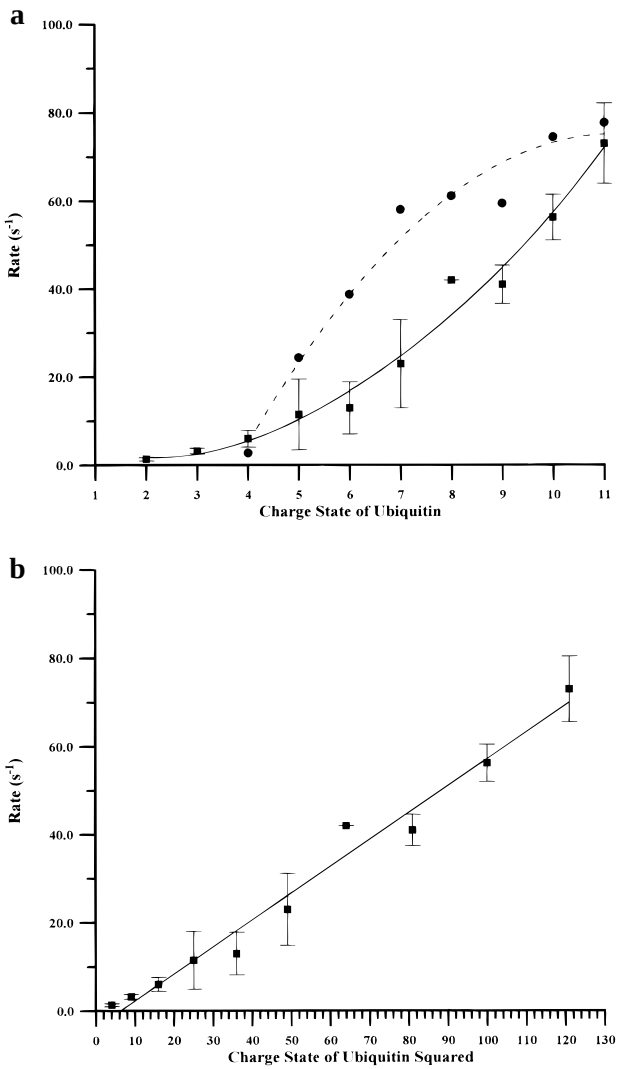

Figure 6. Plot of measured rates vs charge for ion−ion and ion−molecule reaction data: (a) ion−ion data (■) and ion−molecule data (●) adapted from reference 9c and (b) linear dependence of rate vs charged state squared for ion−ion reactions.

giving rise to the data of Figures 4 and 5. While the maximum corrected signal levels of the ubiquitin ions of low charge do not equal the combined intensities of all charge states present at $t = 0$, it is likely that differential detector response could account for at least some of the difference. Although major ion loss is not indicated in the ubiquitin data, we have noted significant losses in signals, even corrected for scan rate, for *m*/*z* values in excess of 30 000. This observation is most likely due to instrumental limitations in ion storage and detection rather than to a fundamental characteristic of ion/ion chemistry.

Figure 6a shows plots of ion/ion and ion/molecule rates for proton transfer as a function of ubiquitin charge state where $n \leq 11$. The ion/molecule reaction data are taken from the work of Cassady et al.[9c] for the base *N*,*N*,*N*′,*N*′-tetramethyl-1,4-diaminobutane (PA = 246 kcal/mol).[23] The ion/molecule reaction data were reported as rate constants and were converted to rates here by multiplying the rate constants by 6.48×10^9 cm^{-3}, the highest number density of the neutral base reported to be used in the ion cyclotron resonance mass spectrometry studies. This was done to allow for direct comparison of the ion/ion and ion/molecule reaction results. We have not developed a means for the accurate measurement of anion number densities during the ion/ion reaction period. Rather than convert the rate data to rate constants using an anion number density estimate, which is accurate only to within an order of magnitude, we simply report the rate. Anion number densities are constant for the measurements so that the reported rates are directly proportional to rate constants.

The rate versus charge state behavior of the ion/ion reactions is clearly very different from that of the ion/molecule reactions. The latter show relatively high reaction rates at high charge states with a relatively abrupt decrease in rate over a few values of *n*. The values of *n* over which the rate decreases rapidly are dependent upon the strength of the base (as reflected in the ion/molecule reaction kinetics not reproduced here associated with weaker bases in the Cassady study[9c]), as expected for a reaction that proceeds over an energy surface like that of Figure 1b. The faster than linear decrease in rate reflects a decrease in reaction efficiency, the fraction of ion/molecule collisions that lead to reaction. Ion/ion reaction rates also show a decrease with charge state but the shape of the curve is very different. Equation 12 predicts a Z^2 dependence for the rate. Figure 6b shows the ion/ion rate data plotted as a function of Z^2 indicating that the predicted behavior is followed. In the absence of accurate anion density information, no quantitative conclusions regarding reaction efficiency can be drawn. However, the linear dependence of rate on Z^2 indicates that the ion/ion reaction efficiency is constant for all charge states, in contrast with the ion/molecule reaction data.

Equation 12 can be used to provide a predicted k_c vs Z_1^2 line which can be used to extract an anion number density of 10^7 cm^{-3} from the data of Figure 6b, assuming a reaction efficiency of unity. This value is well within the range of anion densities expected under the conditions used to measure the ion/ion reaction rates. The pseudo-potential well-depth model of the ion trap[27] predicts a maximum anion density of 10^8 cm^{-3} under these conditions. At longer ionization times, significantly greater reaction rates were noted indicating that the ion density used for the kinetic measurements summarized in Figure 6 was not the maximum anion density that could be maintained in the ion trap. Long anion accumulation times were not used for the kinetic measurements because the high charge state cations disappeared too quickly for reliable rate measurements. Therefore, these reactions may very well be unit efficient, as might be expected for reactions as highly exoergic as these are believed to be.

It is noteworthy that each ubiquitin charge state appeared to react with a single rate constant. Cassady et al. have observed that ubiquitin ions of several charge states display reaction kinetics that are a convolution of two or more reacting populations,[9c,g] depending upon the strength of the base. Such an observation could arise from isomeric forms of the protein. Native and de-natured forms of ubiquitin have been implicated as giving rise to two distinct charge state distributions in electrospray mass spectra with the dominant form being determined by solution conditions.[5d,e] The de-natured α-helix form is expected to dominate under the conditions used in this work. The lack of irregular behavior in the ion/ion versus rate versus charge state data cannot be used to draw conclusions regarding the presence or absence of conformation mixtures of ubiquitin ions in the gas phase. Further studies along these lines are probably warranted. However, based on the preceding arguments regarding the thermodynamics and energy surfaces associated with ion/ion and ion/molecule proton transfer reactions, ion/ion reaction rates are expected to be significantly less sensitive to protein structural differences than are ion/molecule reaction rates.

(27) See: March, R. E.; Hughes, R. J. *Quadrupole Storage Mass Spectrometry*; John Wiley and Sons: New York, 1989; Chapter 3.

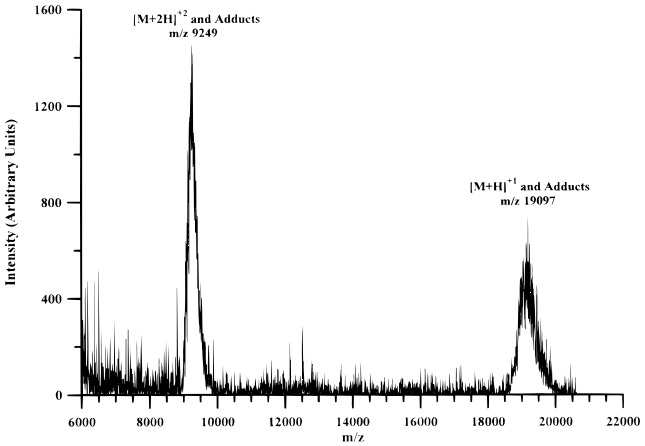

Figure 7. Ion−ion recombination chemistry associated with the anions derived from an air glow discharge when they react with horse skeletal myoglobin. The formation of adduct peaks causes peak broadening and shifts the mass distribution to high *m*/*z* values when compared to the data generated in Figure 3b.

The ion/ion reaction analogy to clustering in ion/molecule reactions is recombination, as represented in the generic reaction

$$MH_n^{n+} + A^- \rightarrow (MH_nA)^{(n-1)+} \qquad (18)$$

Cation attachment to polyanions has been observed in the ion trap.[10d] We have also observed examples of reaction 18 involving multiply-protonated proteins. For example, Figure 7 shows the results of an experiment in which the collection of multiply-charged ions derived from electrospray of myoglobin are subjected to storage in the presence of anions derived from glow discharge ionization of air. A mixture of anions is produced from the glow discharge of air consisting primarily of oxides of nitrogen and carbon.[13,28] In addition to proton transfer, clear evidence for adduct formation is noted by the broadening of the peaks to the high mass side, relative to the spectrum of Figure 3b. We have studied a number of smaller species, such as doubly-charged peptides, and have found that some anions readily attach to peptides/proteins whereas others react principally or exclusively by proton transfer. For example, we have observed that doubly-protonated bradykinin reacts with $SO_2^{\bullet -}$ exclusively by proton transfer whereas both proton transfer and attachment are observed with $SO_3^{\bullet -}$.[25] A full delineation of proton transfer versus recombination chemistry is beyond the scope of this report. However, Figure 7 is intended to illustrate that recombination chemistry can compete with proton transfer in ion/ion reactions. It is also notworthy that the observation of recombination lends support to the notion that ion/ion reactions involving high-mass multiply-charged proteins can proceed through a long-lived collision complex.

(28) Langford, M. L.; Todd, J. F. J. In *Practical Aspects of Ion Trap Mass Spectrometry*; March, R. E., Todd, J. F. J., Eds.; CRC Press: Boca Raton, FL, 1995; Vol. III, Chapter 10.

Conclusions

Ion/ion proton transfer reactions involving multiply-charged proteins can be readily effected in quadrupole ion trap. Reaction rates comparable to or greater than those of exoergic ion/molecule reactions using neutral number densities of up to 10^8 cm^{-3} are observed. Ion/ion rate data show a linear dependence of rate on the square of the protein charge, as predicted based on a simple capture collision model. These results suggest that the ion/ion reactions proceed at constant efficiency at all charge states and can therefore be used to reduce the charge of a gaseous multiply-charged protein to arbitrarily low values. Such a capability is attractive in dealing with ambiguities arising from distributions of multiply-charged ions. Just as with ion/molecule reactions, adduct formation can compete with proton transfer. The anions derived from PDCH have shown no evidence for recombination but a number of other anions have been observed to attach to high mass cations. The factors affecting the competition between charge transfer and recombination are the subject of ongoing studies.

Acknowledgment. J.L.S. acknowledges support through an appointment to the Oak Ridge National Laboratory Postdoctoral Research Associates Program administered jointly by the Oak Ridge Institute for Science and Education and Oak Ridge National Laboratory. This work was supported by the National Institutes of Health under Grant No. R01GM45372. Oak Ridge National Laboratory is managed for the U.S. Department of Energy under Contract DE-AC05-96OR22464 by Lockheed Martin Energy Research Corporation.

JA9611755